Mitochondria in chemical-induced toxicity

Stel, W. van der

New approach methods (NAMs) supporting read-across:

two neurotoxicity AOP-based IATA case studies

Wanda van der Stel, Giada Carta, Julie Eakins, Johannes Delp, Ilinca Suciu5, Anna Forsby, Andrea Cediel-Ulloa, Kristina Attoff, Florentina Troger, Hennicke Kamp, Iain Gardner, Barbara Zdrazil, Martijn J. Moné , Gerhard F. Ecker, Manuel Pastor, Jose Carlos Gomes, Andrew White, Erik H.J. Danen, Marcel Leist, Paul Walker, Paul Jennings, Susanne Hougaard Bennekou[#], Bob van de Water[#]

ALTEX. 2021 Jun; doi:10.14573/altex.2103051

Read-across approaches are considered key in moving away from *in vivo* animal testing towards addressing data-gaps using new approach methods (NAMs). Ample successful examples are still required to substantiate this strategy. Here we present and discuss the learnings from two OECD IATA endorsed read-across case studies. They involve two classes of pesticides –rotenoids and strobilurins– each having a defined mode-of-action that is assessed for its neurological hazard by means of an AOP-based testing strategy coupled to toxicokinetic simulations of human tissue concentrations. The endpoint in question is potential mitochondrial respiratory chain mediated neurotoxicity, specifically through inhibition of complex I or III. An AOP linking inhibition of mitochondrial respiratory chain complex I to the degeneration of dopaminergic neurons formed the basis for both cases, but was deployed in two different regulatory contexts. The two cases also exemplify several different read-across concepts: analogue *versus* category approach, consolidated *versus* putative AOP, positive *versus* negative prediction (i.e., neurotoxicity *versus* low potential for neurotoxicity), and structural *versus* biological similarity. We applied a range of NAMs to explore the toxicodynamic properties of the compounds, e.g., *in silico* docking as well as *in vitro* assays and readouts –including transcriptomics– in various cell systems, all anchored to the relevant AOPs. Interestingly, although some of the data addressing certain elements of the read-across were associated with high uncertainty, their impact on the overall read-across conclusion remained limited. Coupled to the elaborate regulatory review that the two cases underwent, we propose some generic learnings of AOP-based testing strategies supporting read-across.

Keywords: *in vitro*, mitochondrial toxicity, neurotoxicity, PBK-modelling, uncertainty analysis

Introduction

To protect human health, pesticide regulations in Europe (EC 1107/2009) are amongst the most demanding regulations in terms of data requirements [European Parliament and the council, 2009], prescribing *in vivo* mammalian studies [Bennekou et al., 2019]. Even though many pesticides belong to the same pesticidal group, like for example strobilurin fungicides, sulfonyl urea herbicides or pyrethroid insecticides, each of the pesticides still requires a full data package. Pesticide regulation is currently undergoing a Regulatory Fitness and Performance Programme (REFIT) exercise. In this context, the Group of Chief Scientific Advisors to the European Commission recommended that, given the already existing vast amounts of data, read-across approaches are being underutilised across these pesticide groups mainly due to prescriptive data requirements [SAPEA, 2018; EU Scientific advice mechanism, 2018]. In its recent report to the European Parliament [European Parliament and the council, 2020], REFIT estimated that each year up to ~100,000 animals had been used for the testing of pesticides [Busquet et al., 2020]. The use and regulatory acceptance of alternative approaches is crucial to reduce such large-scale *in vivo* vertebrate animal testing in Europe. The US-EPA recently set specific goals towards this end in committing to effectively eliminate mammal testing by 2035 [US-EPA, 2020].

The European Horizon 2020 project EU-ToxRisk aims to provide tools and approaches to replace and reduce animal testing with regard to repeated dose and reproductive toxicity[20]. The EU-ToxRisk project has conducted a series of NAM-supported read-across case studies to explore the utility of these *in silico* and *in vitro* methods to replace *in vivo* testing [Escher et al., 2019]. Read-across is a technique for predicting endpoint information for target substance(s) by using data for the same endpoint(s) from other source substance(s), i.e., by confirming similarity regarding properties relevant for the endpoint in quest between target and source compounds. A total of four case studies were elaborated and reported as integrated approaches to testing and assessment (IATA) and submitted to the OECD IATA Case Studies Project[21]. The case studies underwent rigorous regulatory review by the IATA-project member countries and have been endorsed for publication.

In this paper we present, discuss and compare two of four case studies submitted by the EU-ToxRisk project consortium : *"Identification and characterization of parkinsonian hazard liability of deguelin by an AOP-based testing and read-across approach"* and *"Mitochondrial complex-III-mediated neurotoxicity of azoxystrobin - Read-across to other strobilurins"*. They were chosen since they both involved pesticides groups – respectively rotenoids and strobilurins– and took neurotoxicity as the endpoint with the need for *in vivo* repeat-dose testing described in OECD

guidelines (OECD TG424). The cases studies were recently published on the OECD IATA project website [OECD, 2020a; OECD 2020b]. In addition, both cases are based on an AOP-anchored data-generation strategy supported by physiologically-based kinetic (PBK) modelling. The building of the read-across hypothesis and subsequent testing strategy were to a large extent based on the OECD endorsed AOP *"Inhibition of the mitochondrial complex I of nigra-striatal neurons leads to parkinsonian motor deficits"* [Terron et al., 2018][22].

AOPs represent a sequence of key events (KEs) triggered by chemical exposure, occurring at the molecular, cellular, organ, whole-organism or population level. KEs are causally linked to the adverse outcome (AO), are essential for the progression towards the AO, and should be measurable [Ankley et al., 2010; Villeneuve et al., 2014; Ball et al., 2016]. The OECD runs a programme constructing AOPs and promotes guidance on the use of AOPs in developing IATAs [OECD, 2016], recognizing that AOPs can guide testing of underlying mechanisms, e.g. by using NAMs. In the examples of the two case studies presented here we assembled a battery of *in silico* and *in vitro* NAMs to assess the various KEs in the AOP describing neurotoxicity as a consequence of mitochondrial perturbation. Molecular initiating events (MIEs) interactions were modelled computationally and downstream KEs measured biochemically (e.g., inhibition and perturbation of mitochondrial function and the effects on overall cellular viability, specifically neuronal health). The AOP-based approach was supported by biokinetic and PBK modelling to estimate chemical exposure in the *in vitro* systems and *in vivo*.

Background information

Read-across in the assessment of risk/hazard of pesticides targeting mitochondria
In this manuscript we describe two IATA case studies in which classes of chemicals with a defined mode-of-action (MoA) were assessed for their neurological hazard (table 1).

Read-across complex I inhibition: rotenoids (Case study 1)
There is an anticipated hazard for agrochemicals that inhibit complex I (CI) of the mitochondrial respiratory chain to cause toxicity to the nigrostriatal neurons, leading to symptoms that reflect Parkinson's disease. This relationship has been described in a recently OECD endorsed AOP [Terron et al., 2018][22].

One family of pesticides specifically affecting mitochondrial CI are the rotenoids. Two main marketed rotenoids are rotenone and deguelin, which belong to the so-called class of cubé resin pesticides (the root extract from *Lonchocarpus utilis* and *urucu*). The primary pesticidal MoA of rotenoids is the interference with the electron transport chain in mitochondria. Rotenoids inhibit the transfer of electrons from iron-sulfur centers in CI to ubiquinone. This interference affects the creation of usable

cellular energy in the form of ATP and eventually reduces the number of undesired insects and arachnids on treated plants. A similar mode of action is responsible for the piscicidal activity of cubé resin.

Epidemiological studies have indicated that exposure of workers to rotenone was statistically associated with an increased incidence of Parkinson's disease [Dhillon et al., 2008; Tanner et al., 2011]. Moreover, rotenone is used to induce parkinsonian-like phenotypes in experimental animals [Betarbet et al., 2000] and it was also one of the stressors used in developing the aforementioned AOP. It has been reported that deguelin can induce parkinsonian-like phenotypes in rats [Caboni et al., 2004]. Whether deguelin has the same hazard as rotenone for inducing parkinsonian liability in humans is currently unclear.

Through an analogue-based read-across approach using chemicals with high chemical structure and property similarities and identical MoA, we assessed the likelihood of developing parkinsonian liabilities upon exposure to the target chemical deguelin using NAM-derived information from the source chemical rotenone.

Read-across complex III inhibition: strobilurins (Case study 2)
Another group of pesticides targets mitochondrial complex III (CIII). Mutations in the CIII proteins are linked to neurodegenerative disorders, but until now no neurological liabilities caused by chemical induced CIII perturbation have been observed in human tissue [Conboy et al., 2018; Ghezzi et al., 2011; Kunii et al., 2015; Mordaunt et al., 2015]. The objective of this case study was to establish the absence of this CIII-mediated neurotoxic potential (as detected with a TG424 study [OECD 1997]) upon exposure to a subset of CIII inhibitors using a biological read-across approach assessing toxicodynamic and toxicokinetic NAM data.

The formation of the read-across category in this study was based on the hypothesis that the selected compounds share similar chemical structure, similar pesticidal MoA, a similar toxicophore, and similar neurotoxic potential as the target compound. The compound set for this assessment encompassed members of the strobilurin fungicides family. The synthetic strobilurin fungicides are derived from the naturally occurring strobilurins A and B. The strobilurins bind to the quinol oxidation site of cytochrome b of mitochondrial CIII. The target chemical was azoxystrobin and the source compounds were pyraclostrobin, picoxystrobin, trifloxystrobin, and kresoxim-methyl. They all have a full toxicological data-package according to European legislation. Thus, this case study applies a category approach based on biological similarity, i.e. compounds sharing a common pesticidal MoA and toxicophore. However, although sharing the same toxicophore, i.e. the E-β-metaoxyacrylate group, the chemicals display less structural similarity than the above-described rotenoid family [Bartlett et al., 2002].

Table 1:
IATA report information

Consolidated information on the chemicals selected for the read-across case studies assessing complex I inhibition by rotenoids and complex III inhibition by strobilurins. The table follows the structure of the original IATA documents and is subdivided in purpose and analogue information. Purpose depicts the purpose of both read across case studies, the included chemicals (source and target) and the read-across approach. Analogue information describes chemical-specific information concerning physical/chemical properties, *in vivo* ADME, the coupled AOPs and other relevant information collected from external sources (i.e. everything not assessed *in vitro* described in later sections). # = not measured or no information found in literature.

			RX complex I inhibition: rotenoids	
Purpose	**Purpose**		Hazard identification of Parkinson's disease-associated neurological effects caused by complex I inhibitors	
	Approaches		analogue: one TC and one SC	
	Target Chemical(s) (TC)		deguelin	
	Read across		Biological: complex I inhibitors	
			Chemical: similarity target and source	
	Endpoints		Parkinsonian motor deficit disorders	
	Source Chemical(s) (SC)		rotenone	

			deguelin	rotenone
Analogue information	Physchem data	Chemical structure	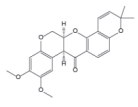	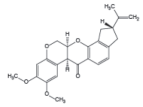
		MW (g/mol)	394,423	394,423
		logP	3.7-5.03	4.1-4.65 (pred.)
		water solubility	1.63e-05 (pred.)	5.07e-07 (exp.)/ 8.79e-06 (pred.)
		Vapour presure	1.26e-07 (pred)	1.08e-07 (pred.)
	In vivo ADME - oral dosing	Absorption	#	High
		Distribution (brain)	#	#
		Metabolism	Extensive	Extensive (pubchem)
		Excretion	High (pubchem)	Extensive
	MoA		Mitochondrial complex I inhibition	
	AOP		Complex I inhibition leads to Parkinson liabilities	
	AOP status		Endorsed by OECD: AOPwiki AOP number 3	
	Chemical/ biological interaction		#	well-described in the AOP
	Alternative assay results		#	well-described in the AOP
	In vivo neurotoxic		# = data gap	yes (AOP nr. 3)

Table 1: IATA report information (continued)

RX complex III inhibition: strobilurins
Flagging for absence of neurotoxicity caused by complex III inhibitors
category: one TC and more SC
azoxystobin
Biological: complex III inhibitors
Chemical: similiarity between strobins, dissimilarity between antimycin and others
Low neurotoxic potential
pyraclostrobin, picoxystrobin, trifloxystrobin, kresoxim-methlyl, antimycin a

azoxystrobin	pyraclostrobin	picoxystrobin	trifloxystrobin	kresoxim-methyl	antimycin A
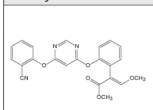	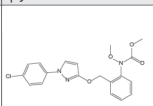	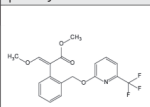	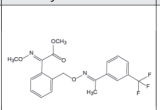	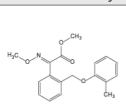	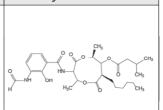
403,394	387,82	367,324	408,377	313,353	548,633
3,7	4,1	3,6	4,9	4,1	4,75
1.26e-05 (pred.)	6.69e-05 (pred.)	2.95e-05 (pred.)	4.56e-06 (pred.)	3.38e-05 (pred.)	#
2,95E-11	5.77e-e9	8,27E-05	3,15E-06	1,06E-06	#
High	Moderate	High	Low	Low	#
Moderate	Moderate	#	Low	Low	#
Extensive	Extensive	Extensive	Extensive	Extensive	#
High	Moderate	Extensive	High	High	#
Mitochondrial complex III inhibition					
Complex III inhibition leads to neurotoxicity					
Proposed AOP based on AOPwiki AOP nr. 3					
Strobilurins bind to the quinol oxidation site (Qo) of cytochrome b of complex III. This prevents the electron flow between cytochrome b and cytochrome c, and petrubs NADH oxidation and ATP production in the mitochondria [Bartlett 2002].					Antimcyin A binds to the Qi side of complex III [Von Jagow 1986]
In vitro data in a variaty of cell types plus measurements in zebrafish demonstrated mitochondrial toxicity [OECD 2020b]. Pearson *et al* reported similar effects at gene expression when comparing pyr and tri exposure to various brain diseases. Azo did not cluster with any brain disease [Pearson 2016].					*In vitro* data showed upon antimycin A exposure mitochondrial dysfunction and neurotoxic effects [OECD 2020b].
# = data gap	no	#	no	no	There are no test guideline neurotox studies. But some in vivo data indicate neurological development defects [Chang 2003].

Existing regulatory *in vivo* data was collected for source and target compounds with a focus on ADME properties and neurotoxicity. The source compounds did not show signs of neurotoxicity in neurotoxic studies nor in other repeated dose toxicity studies. In addition to the strobilurin family members, antimycin A –another well-established CIII inhibitor with neurotoxic effects– was included in the chemical set as a reference compound for the MoA. There is also no direct association between antimycin A exposure and neurotoxicity *in vivo* (including humans), possibly due to the potency and acute toxicity of the compound. Furthermore, no accidental exposures of humans to antimycin A have been reported, but acute exposure of animals to antimycin A indicate symptoms that suggest lethality via neuronal perturbations.

AOPs in the assessment of regulatory questions

Both IATA case studies are built around the endorsed AOP describing parkinsonian liabilities as a result of chemical-induced perturbation of mitochondrial CI [Terron et al., 2018][22] (figure 1A). The risk assessment of the rotenoid family is described completely in relationship to the OECD AOP curated key events. The assessment of the absence of neurotoxicity for the strobilurin family is anchored to a putative AOP adopted from the mitochondrial complex I AOP, with divergence especially at the MIE and AO (figure 1A). The MIE is described as the chemical interaction with and subsequent inhibition of CIII. Since CIII inhibition, like CI inhibition, perturbs the function of mitochondria we hypothesized that this could also lead to neurotoxicity. In the proposed AOP, mitochondrial dysfunction is directly coupled to neuronal degeneration and subsequently neuronal toxicity. The AO is specified as neuronal without a focus on degeneration of the dopaminergic subgroup of neurons in the human brain.

The endorsed and putative AOP have a common fundamental structure consisting of:

- MIE: binding of the chemical to CI/CIII
- KE1: inhibition of CI/CIII
- KE2: mitochondrial dysfunction
- KE3: impaired proteostasis (only included in the endorsed AOP)
- KE4: neuronal degeneration (specifically dopaminergic neurons in the endorsed AOP)
- KE5: neuro-inflammation (only included in the endorsed AOP)
- AO: parkinsonian motor deficits (endorsed AOP) / neuronal dysfunction (putative AOP)

Next, we describe individual KEs assessed by various *in vitro* and *in silico* methods specific for the associated biological processes (figure 1B and C):

A)

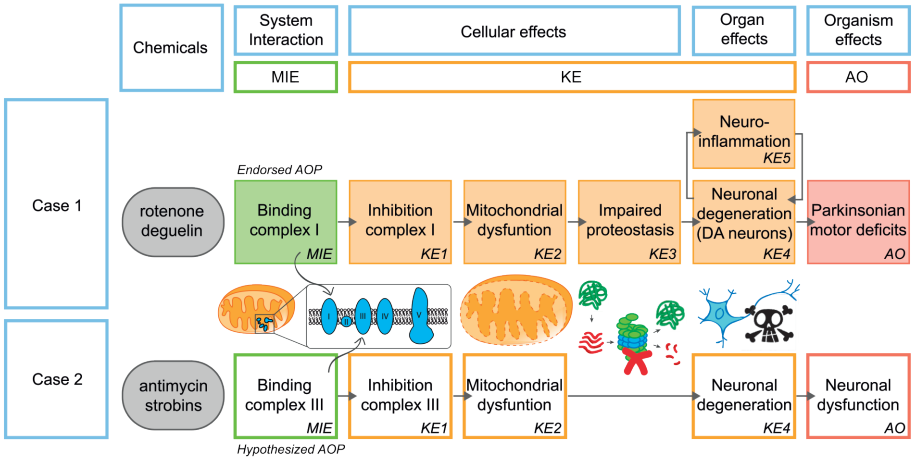

B)

Replace *in vivo*	NAMs available	Difficult to replace

	MIE	KE1	KE2	KE3	KE4	AO
Key event						
Assay	PK studies	Docking studies	Seahorse assay	MMP assay	Protease activity assay	Viability assays Cell death assay	*In vivo* outcome (NA)
	Bioavailability	Similarity studies			Proteosome activity markers	Neuronal health	
Key event						KE5	
Assay						No assay included	

C)

Assay	Type	Measurement	Technique
Pharmacokinetics (PK)	*in silico/ in vitro*	Chemical distribution within a species	Plasma and tissue concentrations were predicted using physiologically based pharmacokinetic (PBPK) models.
Bioavailabiliy	*in silico*	Amount of free chemical in a system	Model predictions (2D steady-state biokinetic model; Fisher 2019)
Docking studies	*in silico*	Probability prediction of binding to a receptor	Model predictions (using Schrödinger software)
Similarity studies	*in silico*	Structural similairty of chemicals	Predictions (2D = Tanimoto score and 3D = USR-CAT)
Seahorse assay (intact cells)	*in vitro*	Mitochondrial respiration	In a seahorse machine: Fluorescent detection of O2 and H+
Seahorse assay (perm. cells)	*in vitro*	Complex specific mitochondrial respiration	In a seahorse machine: Fluorescent detection of O2 and H+
Mitochondrial membrane potential (MMP) assay	*in vitro*	Mitochondrial integrity	Confocal imaging of potential sensitive dye
Protease activity assays	*in vitro*	Degradation of protease substrate	Fluorescent measurement of substrate which becomes visible upon cleavage
Proteosome activity markers	*in vitro*	Expression of CHOP	Confocal imaging of CHOP coupled to GFP
Viability assay	*in vitro*	Viability based on resazurin reduction and ATP level	Assessment of resazurin or ATP levels based respectively on fluorescence and luminescence
Neuronal health	*in vitro*	Neuron outgrowth: length of axons and dendrites	Brightfield imaging of neurons
	in vitro	Neuron degradation: neuronal mass	Brightfield imaging of neurons

Figure 1: AOP explanation with NAMs

A) Schematic representation of the AOPs included in both IATA documents: 1) the endorsed AOP (AOPwiki AOP nr.3) describing Parkinson's defects caused by mitochondrial complex I inhibition, and 2) the hypothesized AOP (based on AOPwiki AOP nr.3) describing neuronal degeneration caused by complex III inhibition. **B)** Table depicting the different assays selected to represent the different key events of the AOPs described in **A**. **C)** Table briefly describing the assays from **B** including type of assay, measurement and technique used.

Methodological considerations

MIE: binding of compound to NADH-ubiquinone oxidoreductase (CI) or cytochrome bc1 complex (CIII): describes the physical allocation of a chemical to the NADH-ubiquinone oxidoreductase (CI) or cytochrome bc1 (CIII) binding pocket. CI of the electron transport chain transfers 2 electrons obtained from NADH oxidation to ubiquinone resulting in its full reduction to ubiquinol [Sharma et al., 2009]. Under normal conditions, CIII of the electron transport chain drives the transfer of electrons from ubiquinol, reduced by CI and succinate dehydrogenase (CII), to cytochrome c [Sarewicz et al., 2015]. Both reactions result in the release of redox energy which is utilized to transport protons from the matrix to the inter-membrane space. The created proton gradient drives the conversion of ADP to ATP by the fifth complex (ATP synthase). The interaction between chemical and receptor can be assessed using docking studies in which the chemical toxicophore of known ligands in combination with crystal structures of the receptor can together provide information on the binding mode and binding efficiency of analogue chemicals. Furthermore, similarity studies based on physical/chemical parameters can provide insights into similarity among chemicals and the likelihood of similarity in binding modes.

KE1: inhibition of NADH-ubiquinone oxidoreductase or cytochrome bc1 complex: describes the interference of the inhibitor with CI or CIII, which leads to a decrease or total inhibition of the reduction reactions needed to contribute to the generation of the proton gradient across the mitochondrial membrane. This proton motive force is used by the ATPase (mitochondrial complex V; CV) to produce ATP, prevention of CV activity leads to the total inhibition of oxidative phosphorylation (OXPHOS). To measure and quantify this KE, the Seahorse bioanalyzer was used to measure oxygen consumption rates (OCR) in permeabilized cells. The system is treated with specific substrates and inhibitors of the electron transport chain, allowing for determination of specific sites of inhibition along the chain.

KE2: mitochondrial dysfunction: the drop in mitochondrial membrane potential (MMP) following CI or CIII inhibition will lead to total malfunctioning of mitochondria. Thus, the cell is stimulated to switch to other sources of ATP production (like glycolysis) to compensate for the OXPHOS-dependent deficiency in ATP.

MMP: Changes in MMP can be monitored with the use of potential dependent fluorescent dyes. Probes such as rhodamine123 or JC-1 accumulate in healthy mitochondria with a polarized membrane. Diminished or changed fluorescence reflect a depolarized MMP as the result of a lost proton gradient over the inner mitochondrial membrane due to electron transport chain inhibition or uncoupling mechanisms (chemically induced or activation of uncoupling proteins).

Oxygen consumption: as a consequence of electron transport chain inhibition, oxygen cannot be reduced to water at the level of complex IV. Changes in OCR (mitochondrial respiration) can be measured *in vitro* using the Seahorse bioanalyzer reflecting the level of inhibition of the target complex upon chemical exposure. Measurements of OCR in intact cells provide a physiologically relevant evaluation of direct effect of chemicals on mitochondrial respiration, as well as information on the bioavailability of chemicals in cells. In addition, measurements of OCR in permeabilized cells help assessing the activity of individual complexes of the mitochondrial electron transport chain.

ATP levels: inhibition of OXPHOS will eventually lead to ATP depletion when neurons can no longer compensate for the required ATP production via glycolysis. The intracellular ATP content after prolonged/repeated exposure can be measured by the luciferin/luciferase luminescence assay.

Effects on glycolysis: as a consequence of perturbation of the mitochondrial respiration, cells will switch to the oxygen-independent glycolysis for ATP production. A measure of this switch is the increase of a glycolysis by-product lactate.

KE3: impaired proteostasis: the direct link between mitochondrial dysfunction and impaired proteostasis is still unclear. Nonetheless, in the case of rotenone-induced toxicity, there is indirect *in vivo* evidence of perturbation of cellular proteostasis. Impaired proteostasis is a complex process. Various cellular perturbations can lead to altered handling of proteins. Two important components include the degradation of proteins through the proteasomal system and the disturbed handling of protein, where the latter may cause a so-called unfolded protein response in the endoplasmic reticulum (ER). Both processes can be quantified in *in vitro* systems using the degradation of a fluorescent surrogate substrate of the proteasome or the expression of protein (DDIT3/CHOP) involved in the ER response upon accumulation of unfolded proteins.

KE4: neuronal degeneration: lack of functional mitochondria ultimately leads to a drop in cellular ATP levels, increased production of reactive oxygen species (ROS), decreased neurite outgrowth, increased neurite degradation and, eventually, induction of cell death mechanisms.

The subsequent effects observed in neurites (mimicking axons and dendrites), i.e. reduced outgrowth or induced degradation, can be visualised based on changes in morphological features of the cell, for instance by quantifying neurite numbers and length in calcein-stained neurons after chemical exposure. Finally, the decreased viability that results from the drop in ATP can be followed using the resazurin-to-resorufin reduction reaction (a reaction dependent on the metabolic status of the

cell). Another option is to assess the number of dead cells using suitable assays, such as propidium iodide staining of nuclei from necrotic cells.

KE5: neuro-inflammation: an inflammatory response to damaged neurons that is characterized by the activation of microglia and astrocytes and the production of pro-inflammatory factors. Persistent inflammation has been observed during the development of parkinsonian liabilities and is thought to contribute to disease progression. In the case studies described here, we did not assess the induction or presence of inflammatory responses. Proper assessment of multifactorial inflammation response requires complex high-level co-culture of multiple cell types, including neurons and glia cells promoting neuroinflammation.

AO: neuronal toxicity: prolonged induction of cell death will in the end manifest itself as neurological dysfunction (e.g. neurodegenerative diseases), and rotenoid-induced CI inhibition specifically leads to parkinsonian liabilities. The development of these multi-factorial and slowly developing neurological diseases are difficult to assess using *in vitro* and *in silico* approaches. AOPs are chemical-agnostic. To implement the endorsed/proposed AOP into a risk assessment context and relate the observed *in vitro/in silico* read outs to the *in vivo* observed toxicological outcome, it is important to consider chemical specific properties and the likelihood that a specific AOP will be triggered. Two important chemical specific aspects were assessed in both case studies: biokinetics and pharmacokinetics.

NAMs used to study MIE and KEs in Case study 1 and 2

Cell models: to assess the likelihood of neurotoxicity upon exposure to rotenoids or strobilurins, we studied the above defined KEs in 4 human cell models using a broad concentration range. The cell models selected for the assessment of the KEs vary per event and include two neuronal cell types (LUHMES and SH-SY5Y cells), a kidney (RPTEC/TERT1) and a liver cell type (HepG2). LUHMES cells are the Lund human mesencephalic cell line differentiated into dopamine-like neurons prior to exposure. SH-SY5Y cells is a human neuroblastoma line demonstrating dopamine-β-hydroxylase activity and can produce relevant neurotransmitters. Both LUHMES and SH-SY5Y cell lines have been used extensively in Parkinson's disease research. RPTEC/TERT1 cells are proximal tubules cells immortalized by a viral integration of hTERT. HepG2 are a hepatocellular carcinoma derived cell line.

***In vitro* assays:** all *in vitro* studies conducted in the 4 different cell models are described in detail in the materials and methods sections of both OECD IATA reports. In summary, LUHMES cells were used to study OCR in permeabilized and intact cells, protease activity (rotenoids only), ATP content, neurite outgrowth, and viability

[Delp et al., 2021]. SH-SY5Y is a human neuroblastoma cell line showing dopamine-β-hydroxylase activity and producing relevant neurotransmitters. Differentiated SH-SY5Y cells were used to study MMP, lactate production, ATP content, neurite degeneration, and viability [Delp et al., 2021]. RPTEC/TERT1 cells are proximal tubules cells immortalized by viral integration of hTERT. RPTEC/TERT1 cells were used to assay for OCR in permeabilized and intact cells, MMP, lactate production, and viability (van der Steel et al., 2020). HepG2 is a hepatocellular carcinoma derived cell line, which we used for measurements of OCR in permeabilized and intact cells, MMP, lactate production, proteasome function (Case study 1), and viability [van der Stel et al., 2020].

Similarity studies: three types of chemical similarity scores were included in the two reports: similarity based on 2D (Tanimoto), 3D, or SMART. The Tanimoto score was calculated for structural fingerprints which were created with RDKIT[23] using MACCS keys to represent the chemical specific SMILES collected from US EPA chemical dashboard[24] and one from CHEMID Plus[25] [Leach et al., 2007; Durant et al., 2002]. 3D shape descriptions were determined using USR-CAT based on 10 conformers collected from RDkit [Schreyer et al., 2012]. Finally, similarity was determined based on common SMARTS patterns[26].

Docking studies: chemical docking for rotenone and deguelin into mitochondrial CI was performed as previously described by Troger *et al.* [Troger et al., 2020].

Biokinetic studies: the relationship between nominal (i.e. added) concentrations in the *in vitro* system and effective concentrations measured in the *in vitro* models, was predicted for all chemicals using an *in silico* model [Fisher et al., 2019]. Measurements of selected chemicals in cells and media were performed for selected chemicals and were compared to *in silico* predictions. Knowledge concerning this relationship between nominal and effective cell concentrations can be used to effectively translate *in vitro* results to *in vivo* conditions (including human).

TK studies: Physiologically based (toxico)kinetic (PBK) models in rat or human were constructed to support the IATA case studies using the Simcyp Simulator V17 (Certara UK Limited, Sheffield) using a previously published approach [Albrecht et al., 2019]. The methodology for PBK modelling was based on approaches outlined in WHO guidelines [WHO, 2010]. In brief, a full body PBK model was used with the lung, adipose, bone, brain, heart, kidney, muscle, skin, gastrointestinal tract and liver described as individual tissue compartments. Local sensitivity analyses were conducted for a number of the input parameters used in the PBK model and the effect of changing the input parameters on the plasma AUC of simulated chemicals was calculated. The specific assumptions for the models can be found in the respective IATA report [OECD, 2020a; OECD, 2020b].

High-content transcriptomics: effects of chemical exposure on gene expression can give valuable information about toxicological MoA, and can also indicate the point-of-departure for toxicity when a level of chemical exposure has a significant impact on the number of differentially expressed genes (DEGs) [Waldmann at al., 2014]. TempO-Seq analyses of approximately 3,600 genes (toxicologically relevant genes plus tissue relevant markers) was performed after exposure of the 4 cell models to rotenoids and strobilurins [Yeakley et al., 2017; Limonciel et al., 2018; Mav et al., 2018].

Results

Read-across complex I inhibition: rotenoids

Assessment of the MIE for rotenone and deguelin was based on *in silico* comparison studies assessing both the docking site and creating a pharmacophore/toxicophore (figure 2, rotenoid, MIE, A&B). The docking approach predicted that rotenone and deguelin have a common binding mode to the NADH-ubiquinone oxidoreductase protein. Furthermore, the created pharmacophore exhibited high similarity for the two chemical structures based on localization of hydrophobic moieties and H-bond acceptors.

Testing for KE1 upon exposure to deguelin and rotenone confirmed that, in LUHMES as well as in HepG2 cells, both inhibitors were selective mitochondrial CI inhibitors (figure 2, rotenoid, KE1, A, B & C and table 2). In both cell lines, rotenone was about 3 times more potent than deguelin in the perturbation of CI. Evaluating CI perturbations based on oxygen consumption readouts revealed that the maximal respiration parameter in intact cells was the most sensitive KE1 readout. Here again rotenone appeared a more potent inhibitor than deguelin.

Potency differences observed in KE1 readouts were also present when assessing mitochondrial integrity as a measure for KE2 (figure 2, rotenoid, KE2, A, B & C and table 2) in SH-SY5Y, HepG2 and RPETC/TERT1 cells. HepG2 and SH-SY5Y revealed a BMC25 for rotenone of about 7-8 times lower than for deguelin. In the case of RPTEC/TERT1 this difference was even a factor of 44. KE1 was also monitored based on the metabolic switch associated with mitochondrial dysfunction. We observed a strongly increased lactate production at lower concentration for rotenone exposure than for deguelin in all tested cell lines (table 2). This effect was most prominent in SHSY5Y cells (rotenone: 0.23 nM; deguelin: 80 nM).

The fourth event (KE3) in the Parkinson's liability AOP describes the perturbation of the proteosome upon chemical exposure. Proteasome activity was assessed based on protease activity and expression of CHOP/DDIT3, a protein involved in impaired protein folding homeostasis responses. Protease inhibition in LUHMES cells displayed similar EC25 values for both deguelin and rotenone (table 2), but rotenone showed a

trend of proteasome perturbation already at lower concentrations (figure 2, rotenoid, KE3, A). Measuring of GFP-CHOP positive HepG2 cells after 24 h exposure showed similar fractions for deguelin and rotenone over the entire concentration range (figure 2, rotenoid, KE3, B). At later time points (48 h and 72 h) a 5-fold difference in GFP-CHOP-positive cells between rotenone and deguelin exposure was observed (figure 2, rotenoid, KE3, C&D and table 2).

The last case study key event (KE4) concerned the measurement of *in vitro* neurite degradation (figure 2, rotenoid, KE4, A&B and table 2) and cell viability (figure 2, rotenoid, KE4, C&D and table 2). Cell viability was assessed based on resazurin reduction in all four models after 24 h of exposure. RPTEC/TERT1 cells demonstrated clear viability perturbation after exposure to deguelin (BMC25 = 398 nM) or rotenone (BMC25 = 102 nM). LUHMES cells demonstrated a viability perturbation upon rotenone exposure (BMC25 = 316 nM) and minimal effects upon deguelin exposure (BMC25 = 9120 nM). Rotenone and deguelin exposures resulted in a slight or no loss of viability in HepG2 and SH-SY5Y cells (for HepG2 and SH-SY5Y, BMC25 > 10,000 nM). We demonstrated that a switch to galactose medium resulted in a clear loss of viability upon exposure to both chemicals, with a lower EC50 value for rotenone [Van der Stel et al., 2020]. The medium switch also resulted in decreased viability for LUHMES cells and SH-SY5Y [Delp et al., 2019].

Effects of chemical exposure on neuronal features were evaluated based on neurite degeneration (measured mean neurite length) in SH-SY5Y or neurite outgrowth (measured neurite area) in LUHMES cells (figure 2, rotenoid, KE4, A&B and table 2). Neurite outgrowth was affected at lower concentrations for rotenone than for deguelin in both cell types. The mean neurite length of SH-SY5Y cells upon deguelin exposure even remained unaffected throughout the used concentration range (up to 10,000 nM).

Read-across complex III inhibition: strobilurins

For this case study a series of source chemicals was defined, including various strobilurin family members. Strobilurins were included for which a full data dossier had been evaluated according to European pesticide regulation (110/2007), yielding picoxystrobin, kresoxim-methyl, pyraclosrobin and trifloxystrobin.

Table 2: Summary of the case studies NAM data.

Summary of data gap filling			**RX complex I inhibition: rotenoids**	
Type of chemical			Target	Source1
Chemical			Deguelin	Rotenone
	Event	Assay		
in silico	Chemical specific	Similarity 3D	structural modeling complex I	structural modeling complex I
		Permeability (*in humans*)	not in report	not in report
		Absorption (*in humans*)	not in report	not in report
		Distribution (*in humans*)	not in report	not in report
		Metabolism (*in humans*)	not in report	not in report
		Excretion (*in humans*)	not in report	not in report

	Key event	Tissue	Assay	Value	
in vivo	AO	Brain	*in vivo* indication	# = data gap	Degeneration nigrostriatal dopaminergic neurons
in vitro	KE1	LUHMES	OCR intact (*)	1,00E+02	2,50E+01
		LUHMES	OCR perm. (*)	8,61E+01	2,64E+01
		Liver	OCR perm. (*)	1,05E+02	3,31E+01
		Liver	OCR intact (b)	1,58E+02	5,01E+01
		Liver	OCR intact (m)	2,57E+01	1,05E+01
		Kidney	OCR intact (b)	1,35E+02	1,35E+02
		Kidney	OCR intact (m)	3,72E+01	2,69E+01
	KE2	Liver	MMP	2,40E+01	3,00E+00
		Kidney	MMP	7,50E+01	1,70E+00
		SH-SY5Y	MMP	3,35E+02	3,45E+01
		Liver	Lactate	1,02E+02	7,50E+01
		Kidney	Lactate	1,91E+02	1,82E+02
		SH-SY5Y	Lactate	<8.00E+01	2,30E-01
	KE3	LUHMES	Protease assay	6,17E+03	6,61E+03
		Liver	Proteosome (**)	4,00E+02	8,00E+01
	KE4	Liver	Viability	> 1.00E+4	> 1.00E+4
		Kidney	Viability	3,98E+02	1,02E+02
		SH-SY5Y	Viability	> 1.00E+4	> 1.00E+4
		LUHMES	Viability	9,12E+03	3,16E+02
		LUHMES	NO	1,15E+03	3,80E+01
		LUHMES	NV	2,09E+04	2,00E+04
		LUHMES	N ATP	4,37E+03	4,37E+03
		SH-SY5Y	ND (24h)	> 1.00E+4	3,20E+01
		SH-SY5Y	N tox (24h)	> 1.00E+4	> 1.00E+4
	Repeat	LUHMES	ND (2x in 10d)	3,98E+02	3,98E+01
		LUHMES	N tox (2x in 10d)	1,26E+03	3,16E+02
		SH-SY5Y	ND (2x in 120h)	3,87E+03	2,65E+01
		SH-SY5Y	N tox (2x in 120h)	3,14E+03	1,22E+02

Table summarizes all data collected through *in silico* and *in vitro* methods (as delineated in figure 2). The table is subdivided in in-silico data, *in-vivo* data collected from existing documentation, and *in-vitro* data. The in vitro data is represented as BMC25 (nM) (exceptions (*) = EC50 and (**) = POD). The values are color coded per read-across case study (red low BMC value, green high BMC value). The color code highlights the concentration relationship for both read-across case studies in which the biological closely related KE 2 and KE 3 demonstrated lower BMC values than KE4 and KE5, echoing the AOP concept that more upstream KEs should happen earlier and at lower concentrations. Tissue types included: neuronal (LUHMES and SH-SY5Y), kidney (RPTEC/TERT1) and liver (HepG2).

Table 2: Summary of the case studies NAM data. (continued)

RX complex III inhibition: strobilurins					
Target	Source1	Source2	Source3	Source4	Reference
Azoxstrobin	Pyraclostrobin	Picoxystrobin	Trifloxystrobin	Kresoxim-methyl	Antimycin A
1,00	0,76	0,65	0,70	0,61	NT
High	High	High	High	High	High
High	Moderate	High	Low	Moderate	Low
Moderate	Moderate	Moderate	Moderate	Moderate	Moderate
Extensive	Extensive	Extensive	Extensive	Extensive	Extensive
Moderate	Low	Low	Moderate	High	Low

Value					
# = data gap	Not detected in acute and repeat-dose neurotox. studies	Not detected in standard repeat-dose studies. No neurotox studies available	Not detected in acute neurotox study and neurotox (evaluation of 90 day repeat study)	Not detected in acute and repeat-dose neurotox. studies	No data
≤ 5.00E+4	≤ 5.00E+4	≤ 5.00E+4	≤ 5.00E+4	≤ 5.00E+4	5,00E+02
≤ 5.00E+4	≤ 5.00E+4	≤ 5.00E+4	NT	NT	NT
> 1.00E+4	3,92E+02	4,02E+03	5,33E+03	6,16E+03	1,89E+01
4,79E+03	4,90E+02	8,32E+02	2,40E+03	5,13E+03	6,70E+00
9,33E+03	7,24E+02	1,12E+03	4,68E+03	2,69E+03	3,39E+00
3,47E+03	4,17E+02	2,00E+03	1,17E+03	> 1.00E+4	2,34E+01
1,82E+03	1,10E+02	1,91E+02	1,91E+03	5,50E+03	4,37E+00
1,12E+03	2,88E+02	3,89E+02	> 1.00E+4	> 1.00E+4	3,00E+00
> 1.00E+4	7,90E+01	> 1.00E+4	2,57E+03	> 1.00E+4	8,00E-01
3,25E+03	2,96E+02	8,32E+03	3,63E+02	1,35E+03	6,60E+01
2,44E+03	1,79E+02	4,75E+02	9,22E+03	1,19E+02	7,20E+01
9,71E+02	2,46E+02	3,31E+02	1,57E+03	> 1.00E+4	1,74E+02
4,89E+03	3,91E+03	7,76E+02	3,16E+03	> 1.00E+4	<8.00E+01
not applicable	not applicable	not applicable	not applicable	not applicable	not applicable
not applicable	not applicable	not applicable	not applicable	not applicable	not applicable
> 1.00E+4	> 1.00E+4	> 1.00E+4	> 1.00E+4	> 1.00E+4	> 1.00E+4
5,01E+03	4,37E+02	8,71E+02	6,03E+03	7,76E+02	3,60E+01
> 1.00E+4	> 1.00E+4	> 1.00E+4	> 1.00E+4	> 1.00E+4	> 1.00E+4
> 5.00E+4	> 5.00E+4	> 5.00E+4	> 5.00E+4	> 5.00E+4	2,57E+04
3,16E+04	1,74E+04	4,90E+04	1,82E+04	4,17E+04	1,74E+04
> 150000	5,25E+04	> 5.00E+4	> 5.00E+4	> 5.00E+4	>12500
1,95E+04	1,51E+04	NT	NT	NT	9,55E+03
> 1.00E+4	> 1.00E+4	> 1.00E+4	> 1.00E+4	> 1.00E+4	1,99E+03
> 1.00E+4	> 1.00E+4	> 1.00E+4	> 1.00E+4	> 1.00E+4	> 1.00E+4
2,51E+04	3,98E+03	1,58E+04	NT	NT	1,00E+04
3,16E+04	7,94E+03	2,00E+04	NT	NT	1,02E+04
> 1.00E+4	3,06E+03	> 1.00E+4	2,07E+03	7,89E+03	4,23E+03
> 1.00E+4	5,02E+03	9,04E+03	> 1.00E+4	> 1.00E+4	3,34E+03

OCR perm. = oxygen consumption rate in permeabilized cells; OCR intact (b) = oxygen consumption rate in intact cells expressed as basal respiration; OCR intact (m) = oxygen consumption rate in intact cells expressed as maximal respiration; N ATP = neuronal ATP levels; N tox = neuronal toxicity; ND = neurite degeneration; NO = neurite outgrowth; NT = not tested; NV = neuronal viability; 2x in 10 d = 2 times repeated exposure in 10 days; 2x in 120 h = 2 times repeated exposure in 120 h.

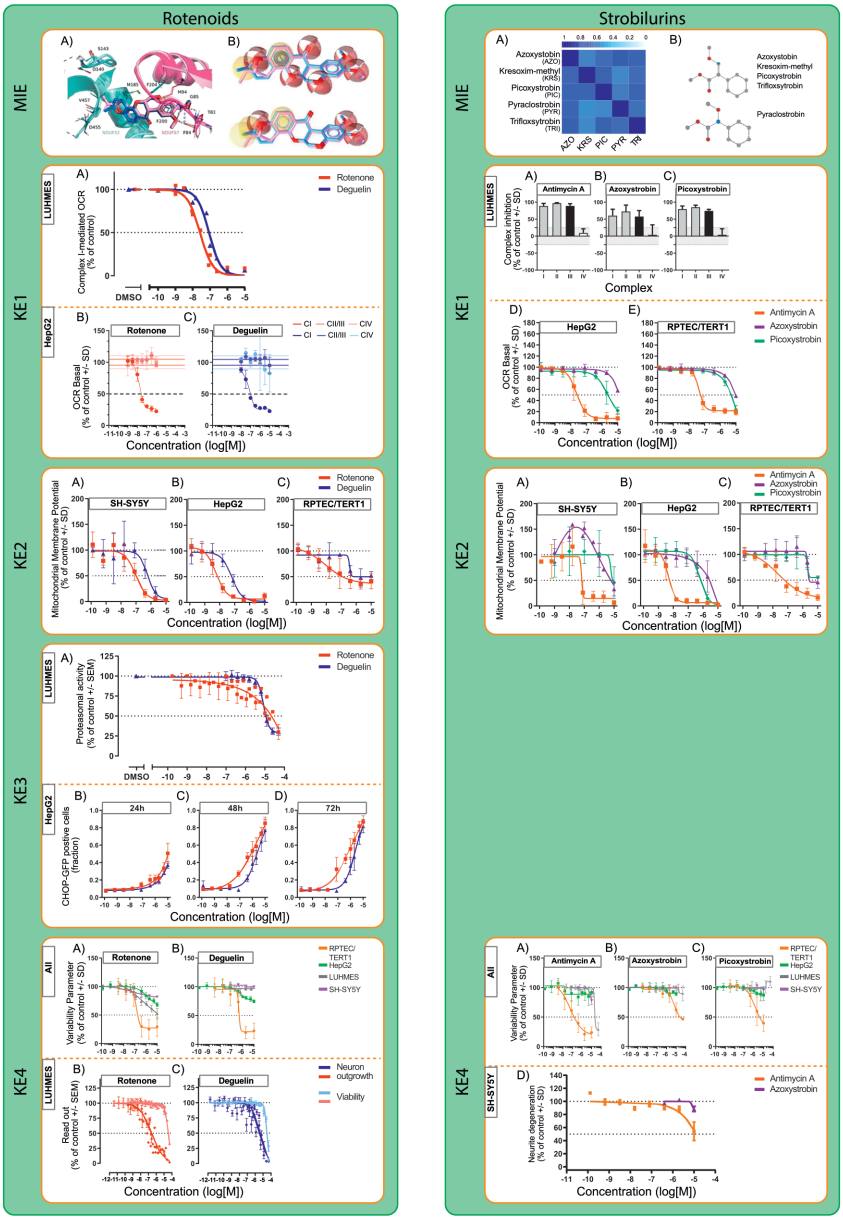

Figure 2: Rotenoid and strobilurin case study represented as neurotoxicity AOP

The figure is subdivided in two green panels describing the AOPs and their KEs for the rotenoid and strobilurin case study, which only KEs assessed in the IATA documents being included. The described data is a representation of all collected data and is linked to the BMC values described in Table 2.

Rotenoids: in all graphs the color scheme described rotenone in red and deguelin in blue, with exception of KE5 A), in which the different represented cells are depicted in 4 colors). **MIE**: **A)** docking study results describing the proposed common binding mode of 1 (pink sticks) and 2 (blue sticks) and **B)** two possible shared pharmacophores of rotenone and deguelin [Troger 2020]. **KE1**: oxygen consumption rate in permeabilized cells. **A)** Mitochondrial complex I inhibition in LUHMES cells after acute exposure to a concentration range of rotenone (red) and deguelin (blue) [Delp 2021]. Mitochondrial CI, CII/III and CIV inhibition in HepG2 after an acute exposure to **B)** rotenone or **C)** deguelin [van der Stel 2020]. **KE2:** mitochondrial membrane potential (MMP) assay. Effect of a concentration

range of rotenone (red) or deguelin (blue) for 24h upon MMP in **A)** SH-SY5Y, **B)** HepG2 or **C)** RPTEC/TERT1 cells [van der Stel 2020]. **KE3:** proteasome perturbation. **A)** Proteasome activity in LUHMES cells upon 24 h exposure to rotenone (red) or deguelin (blue) [Delp 2021]. Fraction of CHOP-GFP positive HepG2 cells upon exposure to rotenone (red) and deguelin (blue) after **B)** 24 h, **C)** 48 h or **D)** 72 h [Van der Stel 2021 unpublished]. **KE4:** neuronal degeneration. Effects on cell viability measured using resazurin reduction in 4 cell lines RPTEC/TERT1 (orange), HepG2 (green), LUHMES (grey) and SH-SY5Y (purple) after 24h exposure to **A)** rotenone and **B)** deguelin [van der Stel 2020, Delp 201]. Effects upon neurite outgrowth and viability in LUHMES cells after 24 h exposure to **A)** rotenone (pink = viability, red = outgrowth) or **B)** deguelin (light blue = viability, blue = outgrowth) [Delp 2021].
Strobilurins = in all graphs the color scheme depicts antimycin A in orange, azoxystrobin in purple and picoxystrobin in green, with exception of KE5 **A)**, in which the different represented cells are depicted in 4 colors. **MIE**: chemical similarity assessment. **A)** 3D similarity score when comparing strobilurin family members represented in a color coded heatmap. **B)** Result of SMART comparison describing structure similarity based on substructures.**KE1:** oxygen consumption rates in permeabilized and intact cells. Complex inhibition assay in permeabilized LUHMES cells after an acute exposure to **A)** antimycin A, **B)** azoxystrobin or **C)** picoxystrobin [Delp 2021]. Effect of an acute antimycin A (orange), azoxystrobin (purple), or picoxystrobin (green) exposure on basal respiration in **D)** HepG2 and **E)** RPTEC/TERT1 cells [van der Stel 2020]. **KE2:** mitochondrial membrane potential (MMP) assay. Effect of 24 h exposure to antimycin A (orange), azoxystrobin (purple), or picoxystrobin (green) upon MMP in **A)** SH-SY5Y, **B)** HepG2 and **C)** RPTEC/TERT1 cells [van der Stel 2020]. **KE4:** neuronal degeneration. Effects on cell viability measured using resazurin reduction in 4 cell lines: RPTEC/TERT1 (orange), HepG2 (green), LUHMES (grey), or SH-SY5Y (purple) after 24 h exposure to **A)** antimycin, **B)** azoxystrobin and **C)** picoxystrobin [van der Stel 2020, Delp 2021]. **D)** Neurite degeneration measured in SH-SY5Y cells after 24 h exposure to antimycin A and azoxystrobin. [Delp 2021].

The likelihood of similar MIEs for the different strobilurin family members was evaluated using *in silico* similarity assessment approaches based on 3D structure and SMART information (figure 2, strobilurin, MIE, A & B and table 2). Comparison of azoxystrobin with the selected strobilurins resulted in comparable 3D similarity scores for all chemicals (ranging from 0.61 to 0.76). This 3D similarity supports the opportunity for performing the read-across. In addition, based on the information contained in the SMART description, we concluded that there is strong conservation of especially the methoxyacrylate moiety within the strobilurin family which also supports our read-across case study.

All performed *in vitro* assays evaluating the following KEs included the target and source chemicals as well as the reference chemical antimycin A. In figure 2 only the results of the target chemical azoxystrobin, source chemical picoxystrobin and reference chemical antimycin A are depicted.

The OCR measured at 50,000 nM in (permeabilized) LUHMES cells confirmed that all chemicals were specific inhibitors of mitochondrial CIII (figure 2, strobilurin, KE1, A, B & C, and table 2). Assessment of CIII-specific inhibition in HepG2 cells demonstrated that pyraclostrobin was the most potent and azoxystrobin the least potent inhibitor (with BMC25 values of 392 nM and > 10,000 nM, respectively) (table 2). Assessment of the effects of chemical exposure on the basal OCR in both HepG2 and RPTEC/TERT1 cells confirmed the potency differences observed in the complex specific assays and the correlated SMART prediction (with pyraclostrobin differing from the others) (figure 2, strobilurin, KE1, D & E and table 2). Furthermore, for both complex-specific and whole-cell assays, antimycin A was a factor 100 to 1000 more effective in perturbing mitochondrial respiration.

Testing for depletion of MMP (KE2) in HepG2, RPTEC/TERT1 and SH-SY5Y after strobilurin exposure also confirmed that pyraclostrobin was the most potent

compound in compromising mitochondrial integrity (table 2). Azoxystrobin and picoxystrobin had similar BMC25 values that were orders of magnitude higher than for antimycin A exposure (figure 2, strobilurin, KE2, A, B &C and table 2).

The final putative KE to be assessed for the strobilurins case study was neuronal degeneration. None of the strobilurins gave rise to a decrease in cell viability in either HepG2, SH-SY5Y nor LUHMES cells (figure 2, strobilurin, KE4, A, B & C and table 2). RPTEC/TERT1 cells showed a decrease in cell viability comparable for azoxystrobin and trifloxystrobin. Exposure to pyraclostrobin, picoxystrobin, and kresoxim-methyl exposure in RPTEC/TERT1 cells resulted in reduced cell viability at ~10-fold lower EC25 than for azoxystrobin. No neuron specific effects (i.e., neurite length differences) were observed after 24 h exposure to strobilurin family members up to 10,000 nM in SH-SY5Y (table 2). In LUHMES cells, effects on neurite outgrowth were observed at higher concentrations, i.e., BMC25 values of 17 and 18 µM for pyraclostrobin and trifloxystrobin and 31, 49 and 42 µM for azoxystrobin, picoxystrobin and kresoxim-methyl, respectively (table 2).

PBK data

Biokinetic and PBK models were developed to support both case studies. Rotenone and deguelin have similar physicochemical properties, being neutral compounds with logP values of ~4. Measured human plasma binding and red blood cell distribution of the compounds, as well as the rate of metabolism in human hepatocytes, was similar. Plasma concentrations of rotenone and deguelin were simulated in both humans and rats using PBK models. The simulated unbound plasma exposure of the two compounds in humans was similar, once more supporting the use of rotenone as a source compound for deguelin. Using an *in silico* estimate of protein binding, the volume of distribution and brain concentrations of deguelin predicted by the PBK model were in reasonable agreement (1.3-fold) with observed rat data [Udeani 2001]. Plasma and brain concentrations of rotenone and deguelin were predicted to be similar in rat (within 1.5-fold) for similar administered doses. The biokinetic model predicted that the distribution of rotenone and deguelin within the different *in vitro* systems would vary from system to system (depending on cell numbers and media composition), but would be similar within each system. The *in silico* biokinetic predictions for rotenone agreed well with experimentally measured values. Overall, the biokinetic and PBK modelling supported that the cellular exposure of the two compounds would be comparable when the same dose was applied.

The strobilurin compounds have a range of lipophilicity values (2.5 – 4.5), with azoxystrobin being the least lipophilic. There was a trend for human plasma protein binding with increased lipophilicity, with azoxystrobin having the lowest protein

binding (highest measured fu). The predicted volume of distribution for the compounds was in the range 0.8 – 3 L/kg in humans with similar values being predicted in the rat [Poulin et al., 2002; Berezhkovskiy et al., 2004; Rodgers et al., 2006]. Steady-state brain to plasma distribution ratio was predicted to be 0.4 to 3.9 in the rat across the series of compounds and between 0.98 and 4.4 in humans. Azoxystrobin was in the middle of the range in both species with brain concentrations being predicted to be about 2-fold of those in plasma in both rat and human.

Using *in vitro* metabolism data in human hepatocytes, *in vitro*-to-*in vivo* extrapolation approaches were used to predict the clearance of the compounds. These values ranged from 0.8 to 44 L/h with azoxystrobin having a relatively high predicted clearance (24.4 L/h). Combining the predictions for the volume of distribution and clearance, azoxystrobin was predicted to have the shortest half-life of the compounds in the case study.

Using an allometric approach to scale down the predicted human clearance the rat pharmacokinetics of the compounds was predicted. For picoxystrobin, trifloxystrobin, kresoxim-methyl, azoxystrobin and picoxystrobin the rat PBK models were consistent with available pharmacokinetic data. At oral doses of 10 and 100 mg/kg the total concentrations of azoxystrobin predicted in the rat were within the range of simulated concentrations of the other compounds. However, when free plasma concentrations were considered, azoxystrobin had the highest unbound Cmax; but due to rapid clearance and short half-life the steady state concentrations were lower than –but similar to– those of picoxystrobin.

In silico biokinetic modelling predicted that the different compounds would have different cell:nominal concentration ratios in the different experimental systems. Predicted cell:nominal concentration ratios were lowest for azoxystrobin, the most polar of the compounds under consideration. There was reasonable agreement between the predicted and observed concentrations of azoxystrobin in the *in vitro* systems.

Repeat dosing

We also considered the necessity of repeated dosing or prolonged exposures for the occurrence of downstream KEs close to the AO, in relationship to the nature of the AO. This is relevant for clinically adverse outcomes like parkinsonian liabilities, which develop as progressive degradation of nigra-striatal dopaminergic brain areas at doses that are not acutely toxic.

Assessment of KE4 following exposure to rotenoids in LUHMES and SH-SY5Y cells (2x exposure, 120 h in total) resulted in similar values for neurite outgrowth compared to single exposures (table 2). However, neurite degeneration was identified in SH-SY5Y cells

upon deguelin exposure in the tested concentration range, which was not observed upon a single 24 h exposure. Notwithstanding, repeated exposure induced cell death at the same concentrations as neurite degeneration where observed (table 2).

For the strobilurins case study repeated exposure yielded a 2 to 4.5-fold increase in sensitivity for the detection of neurite effects in LUHMES cells (table 2). In SH-SY5Y cells, effects on neurite degeneration were within detection range following repeated exposure for all tested strobilurins except for the target chemical azoxystrobin. Only trifloxystrobin had an effect on neuron degeneration at a concentration where viability was not yet affected.

Transcriptomics

Follow-up research on both read-across case studies focused on the incorporation of transcriptomics as a promising additional means for enhancing the performance of AOP-based read-across. For this purpose, transcriptomic profiles were collected following 24 h exposures to a broad concentration range of deguelin, rotenone, antimycin A, azoxystrobin, picoxystrobin or pyraclostrobin in all 4 cell lines (LUHMES, SH-SY5Y, RPTEC/TERT1 and HepG2) (figure 3). A cell biological and toxicological relevant target-gene set of >3300 genes was monitored using targeted RNA sequencing-based transcriptomics using TempO-Seq technology (EU-ToxRisk gene panel is an extended version of panel established by the U.S. NIEHS/NTP) [Mav et al., 2018]. Here we will focus on the overall findings; cell type specific results will be discussed in detail in several separate follow-up publications.

Transcripts were considered differentially expressed between treatment condition and solvent control when the fold-change was above 1.5 or below -1.5 and the p-adjusted value was below 0.05. The obtained differentially expressed gene (DEG) profile upon exposure to both rotenoids and strobilurins revealed a strong potency difference. Neuronal cell lines (LUHMES and SH-SY5Y) did not exhibit transcriptomic changes at low concentrations that impact on mitochondrial function and neurite outgrowth. In contrast, HepG2 and RPTEC/TERT1 cells showed earliest changes in gene expression at low concentrations (nM) coinciding with inhibition of CI and III for the respective compounds. Of relevance, some of these genes affected both in HepG2 and RPTEC/TERT1 were related to the ATF4 responsive program that is known to be activated by inhibition of the mitochondrial respiratory chain inhibition including rotenone [Krall et al., 2021]. This is likely part of an adaptive response program to ultimate restore levels of essential amino acids, in particular asparagine. Given that these ATF4-directed programs were not observed in the neuronal cell lines might provide an explanation for the increased sensitivity of the neuronal cells against mitochondrial respiratory chain inhibitors. Further metabolomics analysis of intracellular amino acids levels in

the neuronal cell lines might substantiate this hypothesis. When focusing on the individual HepG2 and RPTEC/TERT1, an increase in DEGs (up or down) occurs at lower concentrations for rotenone exposure compared to deguelin and for antimycin compared to the strobilurins. This observed pattern correlates with the above-described potency differences in the other *in vitro* assays reflecting the AOP KEs.

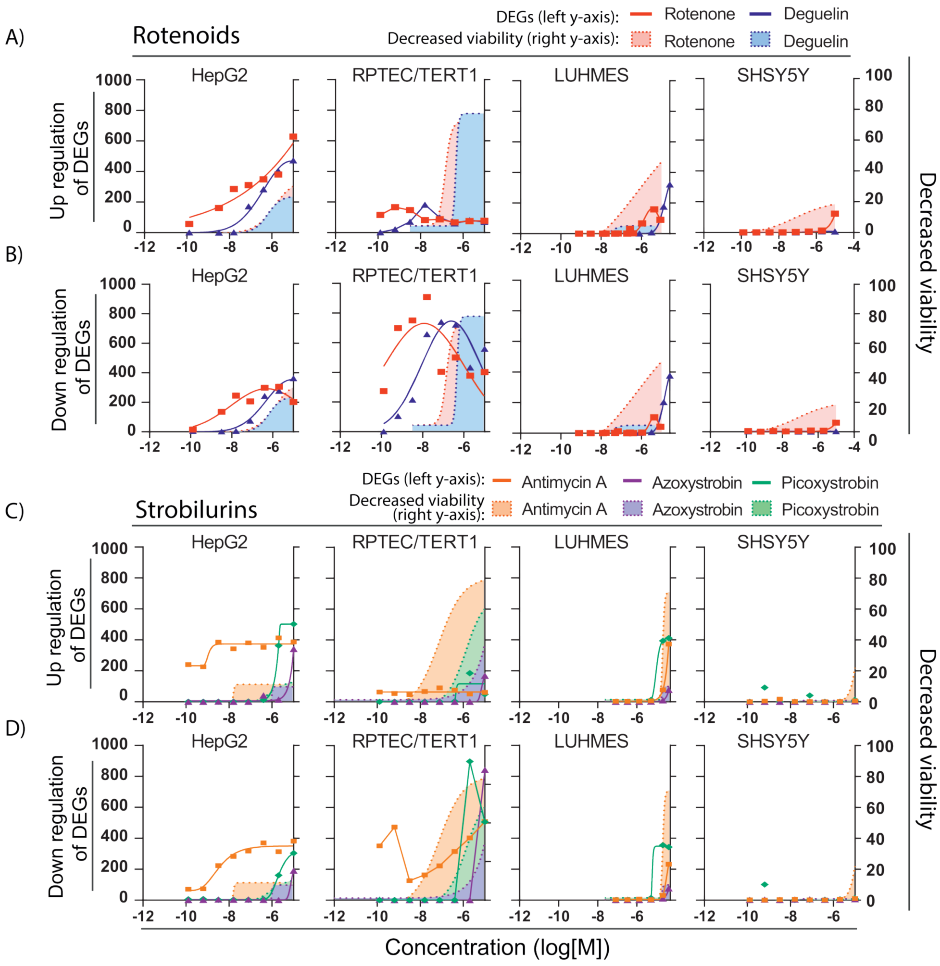

Figure 3: Targeted transcriptomics using TempO-Seq technology for rotenoid and strobilurin treatment in different test systems.

The effects on gene expression measured as the number of differentially expressed genes following 24 h exposures to a concentration range of rotenoids (**A** = up and **B** = down) and strobilurins (**C** = up and **D** = down) in HepG2, RPTEC/TERT1, LUHMES, and SH-SY5Y cells. The chemicals included are for the rotenoids: rotenone (red) and deguelin (blue), and for the strobilurins: antimycin A (orange), azoxystrobin (purple) and picoxystrobin (green). Genes included have a p-adjusted value below 0.05 and a log2FC above or below 2. Colored area under graph represent resazurin viability data (also presented in figure 2 in rotenoids/strobilurins KE5).

Discussion and outlook

This article describes a joint effort to demonstrate the opportunities of performing AOP-based read-across using NAM data with the aim of flagging chemicals for potential neurotoxicity hazards. AOP-based read-across approaches were built around two groups of pesticides targeting mitochondrial complexes, from which we concluded that i) deguelin has a similar MoA as rotenone –but is less potent in its action– allowing for a direct read-across to rotenone to predict parkinsonian liability, and that ii) there is no evidence for a stronger neurotoxic potential of azoxystrobin mediated by a CIII inhibitory MoA as compared to other strobilurins; since source compounds did not show neurotoxicity *in vivo*, it is unlikely that the target compound azoxystrobin is a neurotoxicant via a CIII-mediated mechanism.

The OECD IATA case study template requires a qualitative assessment of the uncertainties for the separate case study elements, conjointly culminating in an overall uncertainty analysis. The various case study elements and their accompanying uncertainties for both the rotenoids and the strobilurins case studies were classified as either low, medium, or high (table 3), as stipulated by the applied 2018 OECD reporting template utilised. This classification pertains to the uncertainty of a used NAM *per se*, but does not explicitly reflect to what extent its result would impact on the overall conclusion of the read-across. Ergo, inclusion of a high-uncertainty methodology may have limited impact on the overall case study conclusions depending on the strength and impact of the other elements/evidence. Practically, based on the experience of the EU-ToxRisk case studies, the OECD IATA Project consortium suggested to discuss the impact of uncertainties on the overall read-across hypothesis and this notion was, in turn, taken up into the OECD template for 2020 [OECD, 2020c]. We will further discuss the main aspects of the uncertainty analysis below.

With one case study relying on an analogy approach and the other on a category approach, the structural boundaries of the read-across by the selected source compounds have different levels of uncertainty. In general, an analogy approach is more uncertain than a category approach which has better defined boundaries based on more negative and positive source compounds.

Table 3: Summary of the uncertainty evaluation of the various test methods applied in the case studies.
The table summarizes the uncertainties identified in both IATA case studies subdivided in 15 categories and scored with low, medium or high uncertainty label. TK = toxicokinetics, TD = toxicodynamics, MoA = mode of action

		RX complex I inhibition: rotenoids		RX complex III inhibition: strobilurins	
Factor		Uncertainty	Comment	Uncertainty	Comment
Structural boundary of the read across		Low/Medium	Hig chemical similarity - but based on an analogue approach with only two compounds	TD = Low	Common toxophore and binding site
				TK =Medium	Substitutions could affect ADME, but *in vivo* and simulations comparable
Mode of action/AOP		Low	OECD endorsed AOP	MoA = Low	strobilurins are desgined to target CIII as their MOA/ AOP putative
				AOP = Medium	
Hypothesis		Medium	Based on endorsed AOP but predictions based on *in vitro* and *in silico* data	Low	Neurotoxic potential established/CIII inducing NT is high. NAMs covering TK/TD support hypothesis
Similarity of source chemicals for read-across		Low	Common toxophore	Low	High 3D similarity with common toxophore
Physical/Chemical properties		Low	Structurally highly similar compounds	Medium	Molecular weight & H-bond similar. Target chemical has a lower logP indicating that less reaches the brain
Toxicokinetics		Low	Metabolism similar/PBPK predictions similar	*in vivo* = Low	*In vivo* data similar
				in silico = low	PBPK predictions similar
Similarity of supportive data	***in vivo***	Low	Regulatory *in vivo* data & human data	Low	Regulatory *in vivo* data
	in vitro	Medium	Not OECD validated – but routine assays in the labs	Medium	Not OECD validated – but routine assays in the labs
Number of analogues		*Not relevant*		Low/Medium	Source compounds demonstrating similar negative results. However, only 1 positive compound which was not similar in structure
Quality of end point data	**Uncertainty of the assay**	Medium	Reported according to ToxTemp/DB-ALM. *In silico* models not validated externally	Low/Medium	Reported according to ToxTemp/DB-ALM. *In silico* models not validated externally
	Following proposed AOP	Low/Medium	AOP endorsed but with the described uncertainties	High	AOP – putative
	KEof the AOPs reflected by assays	Low/Medium	Low uncertainty for all, except proteosomal activity	Medium	Uncertainty whether assays can predict neurotoxicity
Similarity of endpoint data (among source compound(s))		Low/Medium	Similar for all assays except one	Low	No signs of in vivo neurotoxicity of source chemical. High similarity *in vitro* between source and target
Concordance and weight of evidence for justifying the hypothesis		Low	Combined data support that rotenone and deguelin have similar behavior in the various test methods but different potency	Low	The target compound is biologically comparable to the source compounds
Overall		Low	Based on the uncertainty of the above factors and their impact on prediction	Low/Medium	Based on the uncertainty of the above factors and their impact on the prediction

In case of the category-based strobilurins read-across, compounds were all defined by a common toxicophore, although the overall chemical similarity was modest. Unsurprisingly, chemical similarities displayed low Tanimoto scores. However, similarity among the strobilurins was higher when based on the 3D-features of the molecules. This lack of structural similarity was considered unlikely to have significant repercussions on the overall read-across, as biological similarities (TK & TD properties) were comparable. Regarding physicochemical similarities of the strobilurins, the logP of azoxystrobin was lower than that of the source compounds. The impact of this difference was nevertheless assessed as low on the overall read-across conclusion, since the lower logP value would indicate that the compound is less prone to reach the brain in comparison to source compounds with higher logP values.

In case of the analogue-based rotenoid read across, chemical similarity between deguelin and rotenone is high for both structural and physicochemical properties. The similarity between target and source chemicals was further supported by the similarity in the determined pharmacophore and for the CI docking.

In both case studies, uncertainties related to the toxicokinetic behaviour of the compounds were considered low based on *in silico* TK simulations from PBK models. These estimates were further supported by a sensitivity analysis where the impact of the various input values in the PBK model on total plasma AUC in humans and rats was assessed [OECD, 2020a; OECD, 2020b].

As both case studies relied on non-guideline *in vitro* data, formal validation of the assays is not available. This could constitute a high uncertainty. However, most assays were part of a consortium-wide reviewed description document [Krebs et al., 2019] and some were described using DB-ALM documentation [EC, 2019]. All methods were internally validated and assay types are commonly used to address mitochondrial functioning of *in vitro* systems.

Both case studies were built using an AOP as the guiding structure for the selection of assays supporting the assessment of the relationship between MoA (mitochondrial complex inhibition) and adversity (the neurological dysfunction). The uncertainty related to the MoA/AOP is low for the rotenoid case study, as the used AOP has been fully developed and has been endorsed by the OECD; overall AOP uncertainty was gauged as being low[22]. Moreover, one of the stressor compounds for developing the AOP was rotenone, further reducing the uncertainty regarding the relevance of the AOP.

This contrasts the putative AOP on which strobilurins testing strategy relied. The AOP is postulated mainly based on antimycin A data where very little *in vivo* and human data was available [OECD, 2020a; OECD, 2020b]. Notwithstanding, we recently

showed that AOP#3 from AOP-wiki can be expanded to inhibitors of mitochondrial function, specifically CIII inhibitors [Delp et al., 2021].

Several observations were made regarding the approach of linking *in vitro* and *in silico* assays to different KEs of AOPs. When testing for early KEs it is not necessary to use cells directly related to the adverse endpoint in question, if the studied cellular biochemistry was also observed in other cell types (e.g., the mitochondrial respiratory chain). For late KE testing –close to the AO– it is difficult to define "adversity" *in vitro*, using multiple read-outs from different assays reducing the uncertainty. This was exemplified when measuring viability, neurodegeneration and neurite outgrowth, which are all closely related to the human AO as they assess processes related to neuronal integrity.

Also, it has been established that assays used are not only sensitive to mitochondrial toxicity but are also capable of detecting a wide array of MoAs [Delp et al., 2019]. A broad biological coverage of testing is helpful in addressing the question whether other MoAs/AOPs would be needed to be addressed for the read-across. Another observation was, when the hazard concerned an adverse outcome like parkinsonian motor deficits, being an endpoint not routinely picked up in regulatory studies [Ockleford et al., 2017], then an AOP-based read-across approach with robust late KE assays might provide higher confidence than a standard regulatory study, in this case the OECD TG424.

Incorporation of assays monitoring a broader range of possible biological events, like the use of transcriptomics, into an AOP-based read-across could both support the assessment of single KEs or the complete AOP as well as reduce uncertainties originating from other measurement. Firstly, gene expression of individual genes can be linked to the process specific for KEs to assess changes over the length of the AOP. Incorporation of concentration and time factors will help support causal relationship studies. This approach could also be reverted specifically in a read-across context by assessing differences and similarities in gene expression patterns upon exposures to closely related chemicals. The sets of genes can be used as fingerprints for the assessment of other chemicals. Using the approach in the assessment of the gene expression patterns upon exposure to all included CI and CIII inhibitors did not result in the identification of CI or CIII unique genes in HepG2 cells (unpublished Van der Stel). This means that transcriptomics in this particular case would suffice for MIE identification or studies concerning the MIE specifically but rather indicate mitochondrial toxicity in general. Secondly, transcriptomics could support the assessment of a large range of biological pathways that would be activated by mitochondrial toxicants and at multiple levels (sensor, transcription factors and target

genes), which would be labour intensive when done with single assays. We observed no specific modulation of transcriptional programs at low toxic concentrations of the CI and CIII inhibitors in neuronal cells, indicating we likely have not missed unexpected biological perturbations during our assessment. In HepG2 and RPTEC cells transcriptional changes were observed at similar concentrations that affected mitochondrial function.

Previously obtained data provides evidence for the link between our KE4 and the occurrence of neuronal dysfunction and more specifically degradation of dopaminergic neurons in the substantia nigra. The observed specific degradation of neurons originates from a limited capacity to compensate the reduced ATP production by upregulation of glycolysis [Almeida et al., 2001; Almeida et al., 2004; Herrrero-Mendez et al., 2009; Terron et al., 2018]. Moreover, the dopaminergic neurons located in the substantia nigra have a higher energy demand compared to other catecholaminergic neurons in the brain, because of their length, highly branched phenotype and the presence of high numbers of synapses. In addition, they exhibit calcium-dependent autonomous pace-making activity, which has been demonstrated to require more energy than similar activities relying on potassium [Schildknecht et al., 2017]. The combination of this unique architecture and the calcium dependent pace-making activities result in a low residual energy capacity, which makes this cell type very susceptible to cell death caused by a reduction or absence of mitochondrial energy production. At last, hydrophobic toxicants tend to accumulate into the brain, which increases the risk of toxicity upon prolonged low level exposures for neurons.

All together, we have shown that the practical application of an AOP approach through integration of specific technologies and test systems that reflect the AOP MIE and KEs, might find broader application in a read-across safety assessment of structurally related substances.

Based on the learnings from an elaborate OECD IATA case study project regulatory review panel of the two case studies, some more generic learnings on an AOP–based testing strategy supporting read-across can be proposed:

- Anchoring a testing strategy to AOPs is useful since the relevance of endpoints tested is by this means established. When an AOP is not available or it is not well-consolidated, it is necessary to describe and justify the scientific rationale in detail. However, in all cases it is still necessary to address whether other MoAs would be relevant for the problem formulation.
- When testing for a KE, it can be useful to apply different assays to observe consistency, unless one assay has already been established as adequate

- An analogue approach can be justified based on low uncertainty around most of the elements of the read-across.
- A read-across based on not only structural similarity but also biological similarity can be justified by a broad biological coverage of late KE assays together with toxicokinetic data.
- Although, it is recognized that a low toxicity hypothesis is more difficult to underpin (it is difficult to justify when testing is sufficient for regulatory decision-making), it is possible to address this if the problem formulation is narrow and well-defined. In this context, it is useful to provide data on reference compounds to demonstrate that the testing strategy works.

Conflict of interest

The authors declare that there is no conflict of interest

Acknowledgements

This work was supported by the European Union's Horizon 2020 research and innovation programme under Grant agreement no. 681002 (EU-ToxRisk). Parts of this work contributed to two IATA Case Studies projects – *"Identification and characterization of parkinsonian hazard liability of deguelin by an AOP-based testing and read across approach"* – and – *"Mitochondrial complex-III-mediated neurotoxicity of azoxystrobin - Read-across to other strobilurins"* – [OECD, 2020a; OECD, 2020b].